



Universiteit Utrecht

DEBYE INSTITUTE FOR NANOMATERIALS SCIENCE

EMMEPH CENTER FOR EXTREME MATTER
AND EMERGENT PHENOMENA

COLD ATOM NANOPHOTONICS GROUP

Polarization of a Photon Bose-Einstein Condensate

Author:
H.C.Jagers
4029542

Supervisors:
S. Greveling M.Sc
M. Scholten M.Sc
Dr. D. van Oosten

June 15, 2016

Abstract

A Bose-Einstein condensate is a state of matter where bosonic particles macroscopically occupy the ground state of a system. It was predicted as early as 1924 by Satyendra Nath Bose & Albert Einstein. Although this state of matter was deemed possible, it was only experimentally achieved relatively recently. In 1995 by Eric Cornell, Carl Wieman & Wolfgang Ketterle. This Bose-Einstein condensate was made using massive bosonic particles. But all bosons should be able to undergo Bose-Einstein condensation so why not the most common one of them all, the photon?

This question was mostly waved away with a quick reference to the fact that photons adhere to Planck's law. For Bose-Einstein condensation one should be able to tune the temperature and particle number independently. It was thus thought that photons could not be made to condense. This all changed when Martin Weitz showed that he could tune both the temperature and particle number of photons independently by confining them to a white-wall box filled with a medium.

In 2010 they became the first group to achieve a Bose-Einstein condensate of photons. They used an optical dye filled microcavity to make a two-dimensional photon gas Bose-Einstein condense. In 2015 we became the second group in the world to replicate these results.

One of the characteristics of a photon Bose-Einstein condensate that has not yet been researched is its polarization. As Bose-Einstein condensation is an example of spontaneous symmetry breaking. One could expect each condensate to pick a well defined but random polarization. However, slight anisotropy could also force each condensate to pick the same polarization. To answer these questions we build an experimental setup which can measure all four Stokes parameters at the same time. We find that the polarization of every condensate was the same. The polarization of the condensate shows a clear distinction from the polarization of the thermal cloud. We find that the thermal cloud is unpolarized while the condensate is a superposition of multiple polarization states with a strong linear contribution.

Contents

1	Introduction	1
2	Theory	3
2.1	Photon Bose-Einstein Condensation	3
2.2	Polarization	7
2.2.1	Polarization States	7
2.2.2	Stokes Parameters	9
2.2.3	Müller Calculus	10
3	Setup	11
3.1	Construction	11
3.1.1	Schematic	11
3.1.2	Polariser Calibration	12
3.2	Experiment	14
3.2.1	Sequence	14
4	Results	17
4.1	Analysis	17
4.2	Polarization Measurements	18
4.2.1	First Duty Cycle	18
4.2.2	Second Duty Cycle	21
4.2.3	Third Duty Cycle	24
4.2.4	Fourth Duty Cycle	27
5	Conclusion	31
	Acknowledgement	33
	Appendix A Schematic	34
	Appendix B Part List	36
	References	38

1. Introduction

In thermodynamic equilibrium, indistinguishable particles can occupy a set of discrete available energy states in two distinct ways. One way is Fermi-Dirac statistics[1] for particles which obey Pauli's exclusion principle, these are called fermions[2]. The other way is Bose-Einstein statistics for particles that do not obey Pauli's exclusion principle and these are known as bosons[2]. We will focus on the latter case and its implications.

Bose-Einstein statistics was introduced for photons by Satyendra Nath Bose in 1924 and generalized to atoms by Albert Einstein in 1924-1925[3]. They predicted that massive bosons at sufficiently low temperatures or sufficiently high number density would macroscopically occupy the ground state of the system. This phenomenon is a distinct state of matter and is called a Bose-Einstein condensate (BEC). To get massive bosons at sufficiently low temperatures proved difficult and new cooling techniques had to be developed. It took about seventy years to experimentally achieve the first BEC. This was done by Eric Cornell and Carl Wieman in 1995[4].

Considering that photons are bosons it is natural to ask if photons can undergo Bose-Einstein condensation. The difficulty however lies in that photons adhere to the Planck's law[5]. Or in other words the thermal radiation emitted by a body in thermodynamic equilibrium can be approximated by black body radiation. For black body radiation both the spectral distribution of the photon energies and the total photon number depend on the temperature of the body. This means that if we confine the photons using an optical cavity and lower the temperature, instead of occupying the lowest energy modes, the photons get absorbed by the cavity walls. The temperature and total number of photons thus cannot be tuned separately. The conditions necessary to achieve Bose-Einstein condensation can thus not be satisfied.

Different methods have been proposed to achieve number conservation of photons. One of the first processes to be considered was Compton scattering of x-ray photons in plasmas[6]. A different approach was that of photon-photon scattering in a non-linear medium[7-16]. Photons were expected to thermalize by four-wave mixing which can be interpreted as collisions between photons. This process is quite similar to binary collisions of atoms. However in the experimental systems that have been investigated so far, the interactions between photons have proven to be too weak to achieve thermalization.

If we broaden the context of light condensation another type of system can be discussed, the exciton-polariton condensate[17-23]. Exciton-polaritons are bosonic quasi-particles that exist in semiconductor micro-cavities. They consist of a superposition of an exciton and a cavity photon. These particles can undergo condensation if their number density is high enough. However these particles have a lifetime shorter than or equal to that of the thermalization times. So an exciton-polariton condensate has an inherently non-equilibrium nature[23]. However they do exhibit many of the same features that would be expected of a BEC.

The method we are going to focus on in this thesis is that of a number conserving thermalization process of a two-dimensional photon gas in a dye filled microresonator acting as a white-wall box[24–26]. The cavity mirrors provide both a trapping potential and an effective photon mass. This makes the system formally equivalent to a two-dimensional gas of massive bosons inside an harmonic trapping potential. Through multiple absorption- and emission cycles of the photons with the dye molecules, the photons thermalize to the temperature of the dye. The photon energies observed are Bose-Einstein distributed and upon increasing the photon density the phase transition to BEC is observed.

A photon BEC was only recently achieved in 2010 by the research group under the supervision of Martin Weitz[25]. As of 2015 we became the second group in the world to replicate these results. There is still a lot of research that can be done on this subject. One of the characteristics that we are interested in is the polarization state of the photon BEC. Specifically, what is the polarization state and does it change for every newly created photon BEC. The purpose of this thesis is to give a detailed account on how we tried to answer these questions. In Chapter 2 we describe the conditions needed to make a photon BEC and provided the necessary information on polarization. In Chapter 3 the experimental setup is described and in Chapter 4 the results are displayed and discussed. This thesis is concluded with an outlook on future experiments for the polarization of the photon BEC.

2. Theory

2.1 Photon Bose-Einstein Condensation

The theory provided in this section is based upon the work of Martin Weitz[24–26]. Further references will be omitted to prevent redundancy. To create a Bose-Einstein condensate of photons a couple of things are needed: a photon source, a curved-mirror microresonator to provide a trapping potential and a dye for the photons to get into thermal contact with. A representation of such a setup can be seen in Fig.2.1. Here, the dye is held in place by capillary forces. To achieve maximum transmission of the photons through the cavity mirror, we pump under a large angle of 65° with respect to the normal of that mirror. Once inside the cavity, the photons are absorbed and re-emitted multiple times by the dye molecules. This leads to the thermalization of the photons where the resulting photon gas takes over the temperature of the dye solution. When this equilibration of the light to the temperature of the dye is faster than the photon loss in the cavity, the optical spectrum becomes Bose-Einstein distributed. If the number of photons in the cavity surpass a critical number the photons start accumulating in the lower energy states and form a Bose-Einstein condensate.

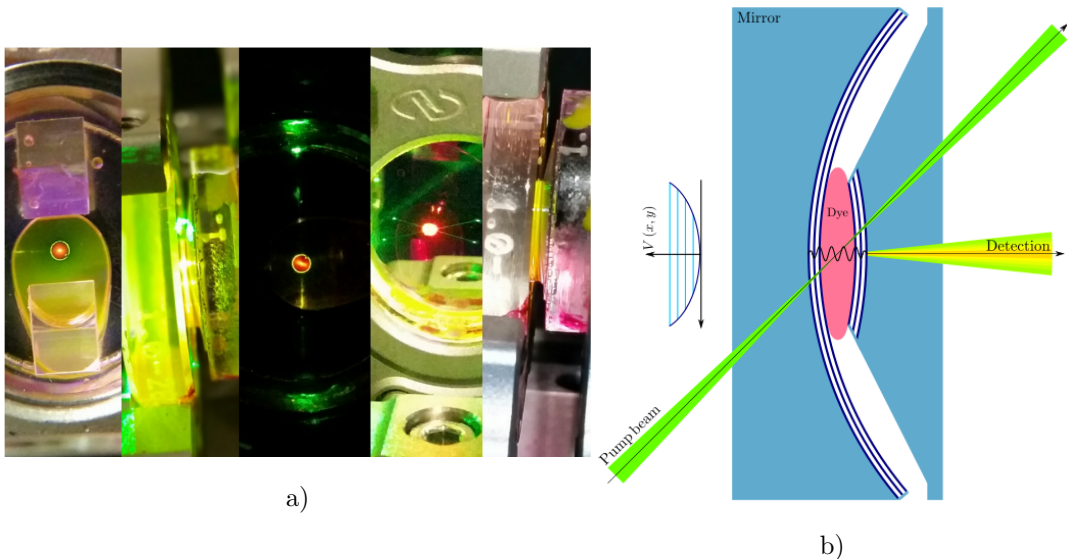


Figure 2.1: a) Pictures of the dye filled cavity taken from multiple angles. The green light is from the pump laser and the yellow light is the fluorescence of the dye. b) This is a schematic drawing of the experimental setup. There are two highly reflective curved mirrors imposing a trapping potential for the two-dimensional photon gas. In between these mirrors there is the dye for the photons to get into thermal contact with and coming in under a angle of 65° there is a pump laser acting as a photon source.

The dye solution used in these experiments is rhodamine 6G dissolved in ethylene glycol with a concentration of $1.5 \times 10^{-3}\text{M}$. Due to the femtosecond timescale of the collisions between the dye and solvent molecules the dye molecules are in a “constant” equilibrated rovibronic state. As a consequence the absorption $\alpha(\omega)$ and fluorescence $f(\omega)$ spectra are linked by the Boltzmann factor $\frac{f(\omega)}{\alpha(\omega)} \propto \omega^3 \exp\left(\frac{-\hbar\omega}{k_B T}\right)$.

This relationship is known as the Kennard-Stepanov relation and gives the photon gas a temperature T .

The mirror separation D_0 of the microresonator is around $1.46 \mu\text{m}$ along the optical axis. A consequence of this is that there is a large frequency spacing between adjacent longitudinal modes which we call the free spectral range. This spacing is comparable with the width of the dye fluorescence which can be seen in Fig.2.2. This leads

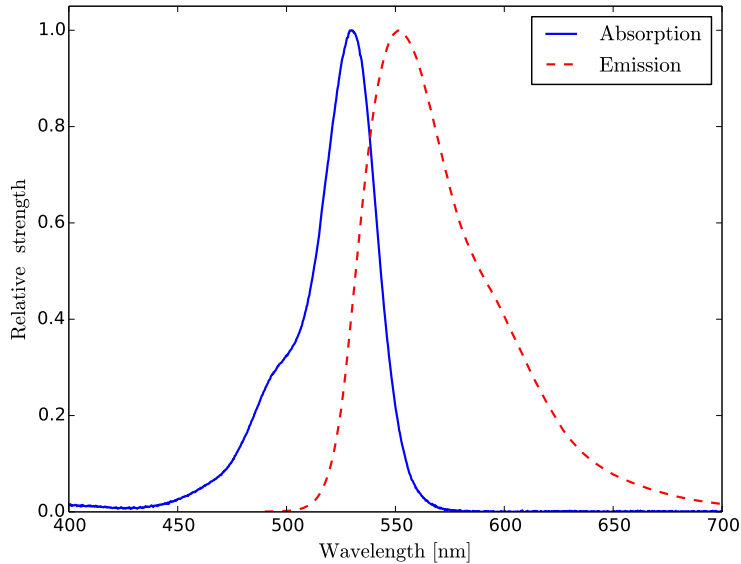


Figure 2.2: Relative absorption and fluorescence strength of rhodamine 6G.

the spontaneous emission to primarily emit photons with the longitudinal mode of $q = 7$. This freezes out one degree of freedom, making the photon gas effectively two dimensional. This establishes a ground state for the photons with a non-vanishing energy, the TEM_{q00} mode.

The photon gas can now formally be described as an ideal Bose gas with a harmonic trapping potential. The energy of a photon in the resonator as a function of the longitudinal wavenumber k_z and transversal wavenumber $k_r = \sqrt{k_x^2 + k_y^2}$ is given by

$$E_{\text{ph}} = \frac{\hbar c}{n} \sqrt{k_z^2 + k_r^2}, \quad (2.1)$$

where c is the speed of light, \hbar is the reduced planck constant and n is the refractive index of the solvent. The boundary conditions yield $k_z(r) = \frac{q\pi}{D(r)}$ where $D(r) = D_0 - 2(R - \sqrt{R^2 - r^2})$ is the mirror separation a distance r from the optical axis and R is the radius of curvature of the mirrors. For a fixed longitudinal mode q and the paraxial approximation ($r \ll R$, $k_r \ll k_z$) Eq. 2.1 can be written as

$$E_{\text{ph}} \simeq \frac{m_{\text{ph}} c^2}{n^2} + \frac{(\hbar k_r)^2}{2m_{\text{ph}}} + \frac{m_{\text{ph}} \Omega^2}{2} r^2, \quad (2.2)$$

with the effective mass defined as $m_{\text{ph}} = \frac{\pi \hbar n q}{c D_0} = \frac{\hbar n}{c} k_z(0) = \frac{\hbar \omega_{\text{cutoff}}}{c^2}$, the trapping frequency $\Omega = \frac{c}{n \sqrt{\frac{D_0 R}{2}}}$ and the ground mode TEM_{q00} acting as the low-frequency

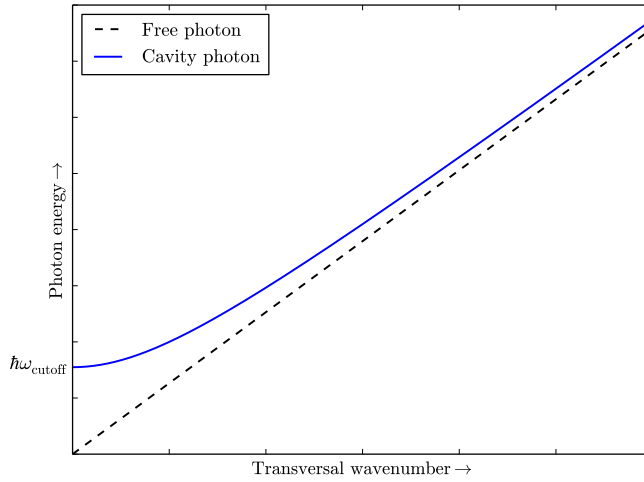


Figure 2.3: Dispersion relation of photons in the cavity (solid line), with fixed longitudinal mode number ($q = 7$), and the free photon dispersion (dashed line).

cutoff ω_{cutoff} .

Eq.2.2 is identical to the energy-momentum relation of a non-relativistic massive particle in a harmonic trapping potential in two dimensions. This equation is shown in Fig.2.3. Because of this we treat the photon as massive bosons in a harmonic oscillator, of which we know the textbook solutions. Using the standard quantization procedure it can be shown that the degeneracy $g(u)$ can be written as

$$g(u) = 2 \left(\frac{u}{\hbar\Omega} + 1 \right), \quad (2.3)$$

with u the transversal photon energy defined as $u = E_{\text{ph}} - \frac{m_{\text{ph}}c^2}{n^2} - \hbar\Omega$. The thermodynamics of a two dimensional Bose gas in a harmonic potential is well understood and shows a phase transition to a BEC at low temperatures or higher number densities. The average number of photons occupying a state with transversal energy u is given by the Bose-Einstein distribution

$$n_{T,\mu}(u) = \frac{g(u)}{\exp\left(\frac{u-\mu}{k_B T}\right) - 1}. \quad (2.4)$$

The chemical potential μ of the photons is defined by

$$N_{\text{ph}} = \sum_u n_{T,\mu}(u), \quad (2.5)$$

with N_{ph} the total photon number. With Eqs.2.2-2.5 it can be shown that the number of photons in transversally excited resonator states saturate at a critical particle number given by

$$N_c = \frac{\pi^2}{3} \left(\frac{k_B T}{\hbar\Omega} \right)^2. \quad (2.6)$$

For our experiment the trapping frequency is of the order $\Omega \simeq 10^{11}$ Hz and we work at room temperature thus $T = 300$ K. This leads to a critical number of $N_c \simeq 10^5$. If the total number of photons is increased beyond this critical number a macroscopic occupation of the ground state is observed. Or in other words a photon BEC is created. This can be seen in Fig.2.4 which shows the spatial radiation distribution of the photons inside the cavity. In Fig.2.4a) the number of photons is below the critical photon number. In this case we do not reach BEC. However, we do observe the thermalized photon gas. The influence of the harmonic trapping potential can be observed from the fact that away from the centre of the trap, the wavelength of the photons are blue shifted. This corresponds to a higher energy. When the photon number is increased beyond this critical number we obtain BEC as is observed in Fig.2.4b). Here, the BEC is characterized by the bright yellow cherry pit at the centre of the trap.

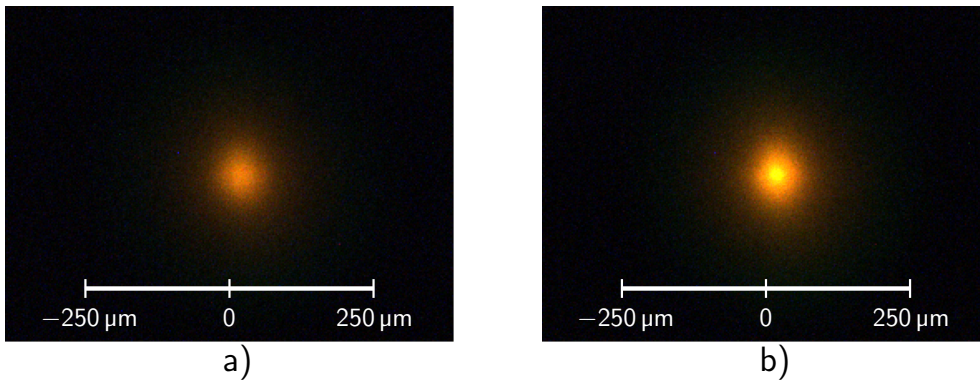


Figure 2.4: Images of the spatial radiation distribution. In a) it is below the critical particle number. Here we only observe the thermalized photon gas. In b) it is above the critical particle number. Here we observe BEC, it is characterized by the bright yellow cherry pit in the centre of the trap.

2.2 Polarization

2.2.1 Polarization States

Polarization is a property of a transversal wave and is defined as the direction in which the electric field vector of the wave oscillates. First we need a coordinate system to determine the polarization state of a wave. Convention is to have the z -axis parallel to the propagation direction[27] and to have the electric field vector $\vec{\mathbf{E}}$ oscillate in the $x - y$ plane as is shown in Fig.2.5. This figure shows an electromagnetic wave propagating in the \mathbf{z} direction with the electric field vector $\vec{\mathbf{E}}$ oscillating in the \mathbf{y} direction and the magnetic field vector $\vec{\mathbf{B}}$ oscillating in the \mathbf{x} direction.

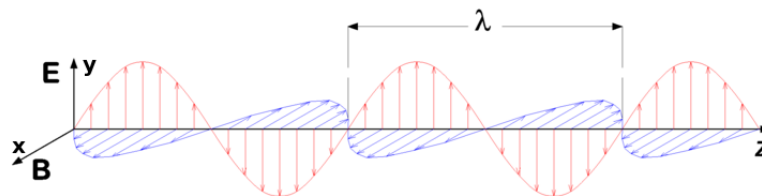


Figure 2.5: An electromagnetic wave travelling in the \mathbf{z} direction with wavelength λ . The electric field vector $\vec{\mathbf{E}}$ (red) is oscillating in the vertical direction. The magnetic field vector $\vec{\mathbf{B}}$ (blue) is oscillating in the direction perpendicular to $\vec{\mathbf{E}}$.

With this coordinate system the we can describe the electromagnetic wave as follows[27]

$$\vec{\mathbf{E}}(\mathbf{r}, t) = \begin{pmatrix} E_x^0 \cos(kz - \omega t) \\ E_y^0 \cos(kz - \omega t + \delta) \\ 0 \end{pmatrix}, \quad (2.7)$$

$$c\vec{\mathbf{B}}(\mathbf{r}, t) = \hat{\mathbf{z}} \times \vec{\mathbf{E}}(\mathbf{r}, t) = \begin{pmatrix} -E_y^0 \cos(kz - \omega t + \delta) \\ E_x^0 \cos(kz - \omega t) \\ 0 \end{pmatrix}. \quad (2.8)$$

With Eqs.2.7 and 2.8 as the electric and the magnetic field vector respectively. Here, c is the speed of light, k is the wave number and $\omega = ck$ is the angular frequency. E_x^0 and E_y^0 are the amplitudes that obey the relation $|\vec{\mathbf{E}}|^2 = (E_x^0)^2 + (E_y^0)^2$ and δ is the phase difference.

Now the amplitudes and phase difference can be used to describe the polarization state of an electromagnetic wave. The wave in Fig.2.5 for instance has an electric field vector that is zero in the x -direction and non-zero in the y -direction. Therefore $E_y^0 \neq 0$ and $E_x^0 = 0$ and the phase $\delta = 0$. So in this instance the wave is linearly vertically polarized (LVP). If $E_x^0 = E_y^0 \neq 0$ and $\delta = 0$ then it is linearly polarized at 45° (L+45P) because the x and y part of the electric field vector are equally strong and are in phase. The resulting vector makes an angle of 45° with the x -axis.

If $E_x^0 = E_y^0 \neq 0$ and $\delta = \pm 90^\circ$ the wave is circularly polarized as is shown in Fig.2.6. In this case the x and y component of the electric field vector are equally strong but

90° out of phase. The electric field vector of these waves never becomes zero but rotates around the z -axis. A circular polarized wave is considered to be right-handed if it rotates clockwise when viewed by the receiver and left-handed otherwise.

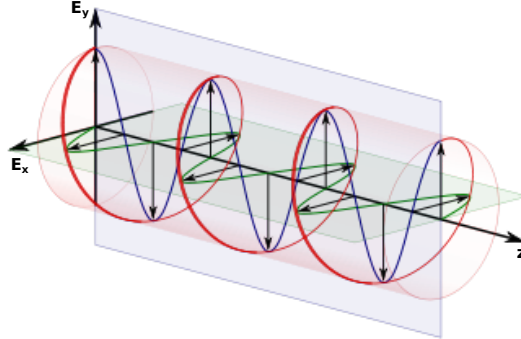


Figure 2.6: A circular polarized wave (red) is the sum of two linear polarized waves (blue and green) 90° out of phase.

All other possible values for E_x^0 , E_y^0 and δ correspond to an elliptically polarized wave. It is called elliptically because viewed by a receiver at a fixed point on the z -axis the electric field vector traces out an ellipse in the $x - y$ plane. The first three examples can also be considered special cases of elliptical polarization. Fig.2.7 shows the so called polarization ellipse and is a way to display the polarization of a wave[28]. The angle ψ is the rotation angle and χ is the ellipticity angle. LVP light has $\psi = 90^\circ$ and $\chi = 0^\circ$, L+45P has $\psi = 45^\circ$ and $\chi = 0^\circ$ and right handed circular polarized (RCP) light has $\psi = 0$ and $\chi = 45^\circ$.

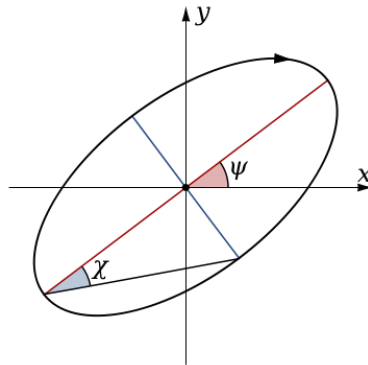


Figure 2.7: At a fixed point in space the electric field vector \mathbf{E} traces out an ellipse in a plane perpendicular to the propagation direction ($x - y$ plane). This polarization ellipse is used to describe the polarization of an electromagnetic wave. Ψ gives the orientation of the semi-major axis with the x -axis where χ gives the arctan of the ratio between the semi-major and semi-minor axis.

A big limitation of the polarization ellipse however is that the rotation angle ψ and the ellipticity angle χ can not be measured directly.

2.2.2 Stokes Parameters

An alternative way to describe the polarization state is to use the Stokes parameters[28–30]. These are a set of four parameters that are observables of the electromagnetic radiation and are defined as

$$\begin{aligned}
 S_0 &= I_{\text{tot}} = I_{0^\circ} + I_{90^\circ} = I_{45^\circ} + I_{135^\circ} = I_L + I_R, \\
 S_1 &= I_{0^\circ} - I_{90^\circ}, \\
 S_2 &= I_{45^\circ} - I_{-45^\circ}, \\
 S_3 &= I_L - I_R,
 \end{aligned} \tag{2.9}$$

where I_{tot} is the total intensity, I_θ is the intensity of the light after it passed through a linear polariser. Here θ denotes the angle the transmission axis makes with the x -axis and is measured in degrees. The intensity of left-handed and right-handed circularly polarized (LCP & RCP) light are denoted by I_L and I_R respectively.

The meaning of the first Stokes parameter S_0 is the total intensity. The second Stokes parameter S_1 describes the preponderance of linearly horizontally polarized(LHP) light over linearly vertically polarized light. Or in other words how much more LHP light there is compared to LVP light. The third Stokes parameter S_2 describes the preponderance of linear polarized light at 45° (L+45P) over linear polarized light at -45° (L-45P). Lastly, S_3 describes the preponderance of LCP light over RCP light. The Stokes parameters also contain two useful properties the first being that if two waves with the same wavevector \vec{k} have identical Stokes parameters, the waves are identical[28]. The second is if several independent waves propagating in the same direction are superimposed, the Stokes parameters of the resulting wave is the sum of the Stokes parameters of the individual waves[28].

The Stokes parameters can also be used to reconstruct the polarization ellipse introduced in the previous section using the following relations[29]

$$\begin{aligned}
 S_0 &= I, \\
 S_1 &= Ip \cos(2\psi) \cos(2\chi), & p &= \frac{\sqrt{S_1^2 + S_2^2 + S_3^2}}{S_0}, \\
 S_2 &= Ip \sin(2\psi) \cos(2\chi), & 2\psi &= \arctan\left(\frac{S_2}{S_1}\right), \\
 S_3 &= Ip \sin(2\chi), & 2\chi &= \arctan\left(\frac{S_3}{\sqrt{S_1^2 + S_2^2}}\right).
 \end{aligned} \tag{2.10}$$

With I the intensity of the radiation, p the degree of polarization which is constrained between $0 \leq p \leq 1$. The angles ψ and χ are the rotation angle and ellipticity angle respectively which are the same angles defined in Section 2.2.1.

Also a common way to represent the Stokes parameters is to use the Poincaré sphere[31] shown in Fig.2.8. The Poincaré sphere is a graphical tool that allows for representation of polarization states in three-dimensional Euclidean space. Each polarization state can be uniquely represented by a point on or within this sphere. On the three axis are the last three normalised Stokes parameters.

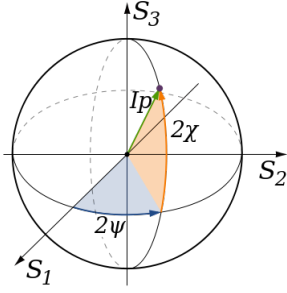


Figure 2.8: A Poincaré Sphere is a parametrization of the last three Stokes parameters.

2.2.3 Müller Calculus

A common practice is to combine the Stokes parameters into a Stokes vector[30]

$$\vec{S} = \begin{pmatrix} S_0 \\ S_1 \\ S_2 \\ S_3 \end{pmatrix}. \quad (2.11)$$

An advantage of doing so, is that they can be manipulated using Müller calculus[30]. Müller calculus is a matrix method which describes the effect of optical elements. If a beam of light is initially in state \vec{S}_i and passes through an element described by Müller matrix M it will come out in \vec{S}_0 . This is written as $\vec{S}_0 = M \cdot \vec{S}_i$. If the light passes through multiple optical elements it is written as such $\vec{S}_0 = M_3 M_2 M_1 \vec{S}_i$. Note that $M_3 M_2 M_1 \vec{S}_i \neq M_1 M_2 M_3 \vec{S}_i$.

Below are listed the Müller Matrices of two common optical elements. There is the general linear polariser

$$\frac{1}{2} \begin{pmatrix} 1 & \cos(2\theta) & \sin(2\theta) & 0 \\ \cos(2\theta) & \cos^2(2\theta) & \sin(2\theta) \cos(2\theta) & 0 \\ \sin(2\theta) & \sin(2\theta) \cos(2\theta) & \sin^2(2\theta) & 0 \\ 0 & 0 & 0 & 0 \end{pmatrix}, \quad (2.12)$$

with θ the angle between the transmission axis and the x -axis and the general linear retarder

$$\begin{pmatrix} 1 & 0 & 0 & 0 \\ 0 & \cos^2(2\theta) + \cos(\delta) \sin^2(2\theta) & \cos(2\theta) \sin(2\theta) - \cos(2\theta) \cos(\delta) \sin(2\theta) & \sin(2\theta) \sin(\delta) \\ 0 & \cos(2\theta) \sin(2\theta) - \cos(2\theta) \cos(\delta) \sin(2\theta) & \cos(\delta) \cos^2(2\theta) + \sin^2(2\theta) & -\cos(2\theta) \sin(\delta) \\ 0 & -\sin(2\theta) \sin(\delta) & \cos(2\theta) \sin(\delta) & \cos(\delta) \end{pmatrix}, \quad (2.13)$$

with δ the phase difference between the slow and fast axis and θ is the angle of the fast axis compared to the x -axis.

3. Setup

The purpose of the setup is to determine the polarization of a photon BEC. As described in Section 2.2.2 a way to do this is to determine the Stokes parameters. This can be done by intensity measurements. The difficulty in this however lies in the lifetime of 500 ns of the photon BEC. Standard ways to measure polarization will not work in this case because these depend on a continuous light source[32]. A way to overcome this obstacle is to measure the necessary intensities all at the same time with a sensitive camera.

3.1 Construction

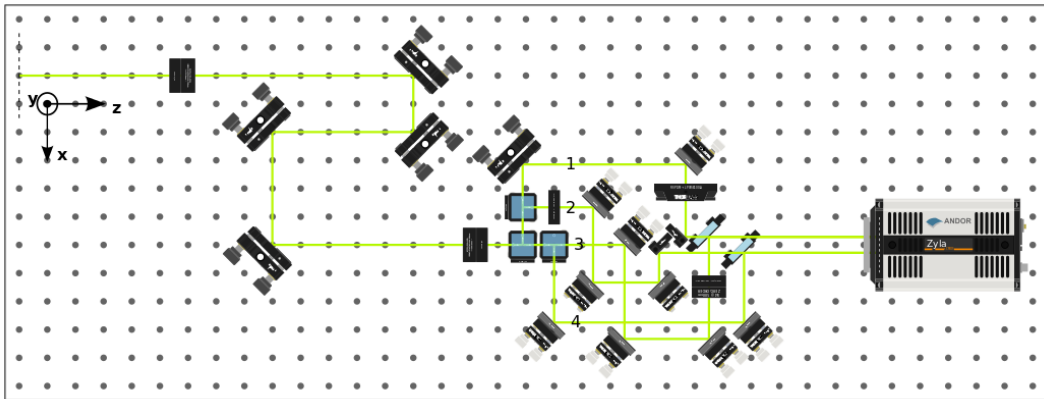


Figure 3.1: The setup used to measure the polarization of light coming of the photon BEC. The light comes in from the top left and passes through two lenses to enlarge the image. The light then passes through a series of beam splitters to split the light into four equal beams. All four beams have an equal path length and pass through different optical elements before being projected on the camera.

3.1.1 Schematic

Fig.3.1 shows the setup used for the polarization measurements. In this setup the x -axis is defined as being parallel to the surface of the table and the y -axis is normal to this surface. The z -axis is along the direction of propagation.

The signal of the photon BEC is too narrow to make an image with a satisfactory resolution on the camera that is used. Therefore we magnify the image five times by directing it through two lenses with focal lengths 150 mm and 500 mm. This ensures that we see ample details of the BEC. The mirrors in between the two lenses are used to make the setup more compact. After the image is magnified it is equally divided over four paths using three non polarizing beam splitters. All four paths have roughly the same length and pas through different optical elements.

Path 1 is first raised by 6 mm with respect to the height before passing through the beam splitters. The beam then passes through a linear polariser oriented 0° compared to the x -axis. After this it is reflected using a D-mirror onto the top left corner of the camera. This yields I_{0° .

Path 2 passes through a linear polariser oriented 45° compared to the x-axis and is reflected in the top right corner of the camera. This beam is also raised 6 mm and yields I_{45° .

Path 3 passes through a quarter waveplate with its fast axis oriented 0° compared to the x-axis. This will transform LCP and RCP in L+45P and L-45P respectively. It then passes through a linear polariser oriented -45° compared to the x-axis. This means it is oriented 135° compared to the fast axis of the quarter waveplate thus this yields I_R . This path is reflected onto the bottom left corner of the camera

Path 4 is not passed through any polarity optics, this yields I_{tot} and it is reflected onto the bottom right corner.

3.1.2 Polariser Calibration

To calibrate the linear polarisers in the setup of Fig.3.1 we use a He-Ne laser. Using a polarizing beamsplitter we make sure that the light is polarized 0° with respect to to the x -axis. The linear polarisers in path 1 and 2 are placed in rotation mounts, a powermeter is placed behind the rotation mount and the mount is set at 0° . This mount is then rotated 360° in steps of 5° . At each step the power is recorded and a sine function is fitted to the data for both polarisers. The results are shown in Fig.3.2. Using these results the rotation mount in path 1 will be set at $36.5^\circ \pm 0.5^\circ$ for maximum transmission and in path 2 it will be set at $63.5^\circ \pm 0.5^\circ$ for exactly half of the maximum transmission.

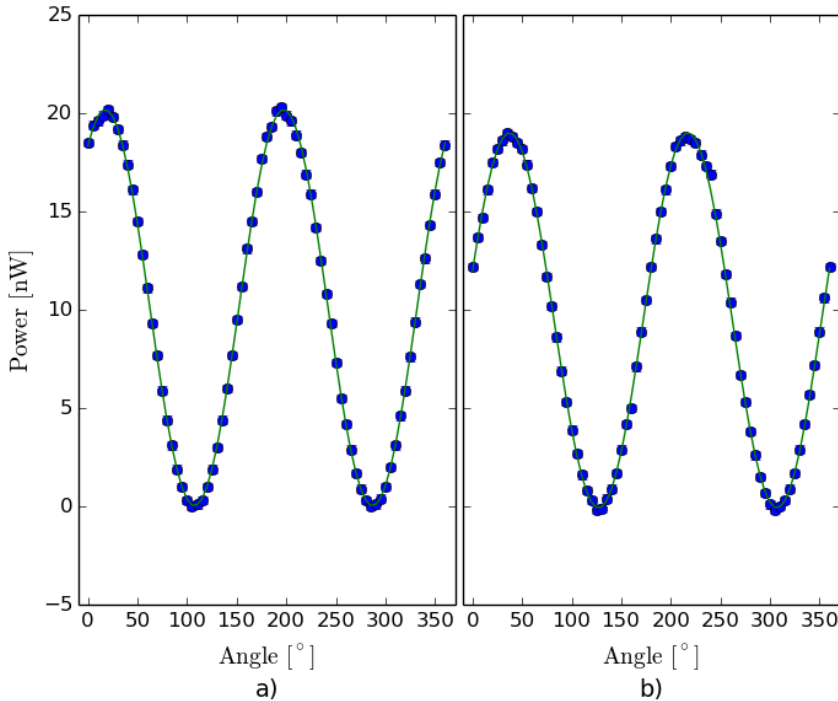


Figure 3.2: Results of the polariser calibration measurement for path 1 a) and for path 2 b).

To calibrate the quarter waveplate and the linear polariser in path 3 a powermeter is placed in this path. First the power is measured with neither of these optical elements. Then the linear polariser is placed in a lens holder and inserted into the path. The polariser is then rotated clockwise until only half of the original power is measured because this means the linear polariser makes an angle of $\pm 45^\circ$ with the x-axis or -45° in our case. Then the quarter waveplate is inserted. This element has lines indicating the fast axis so initially it is placed horizontally to the x-axis using visual indications. To make sure it is placed correctly the powermeter is used. If the quarter waveplate is indeed placed horizontally than it should have no influence on the power. Because a waveplate only slows down the part of the electric field vector that is perpendicular to its fast axis. Or using the Müller calculus from Section 2.2.3, the incoming Stokes vector is $\vec{\mathbf{S}} = (1 \ 1 \ 0 \ 0)^\top$ and the Müller Matrix of the quarter

waveplate is $M = \begin{pmatrix} 1 & 0 & 0 & 0 \\ 0 & 1 & 0 & 0 \\ 0 & 0 & 0 & -1 \\ 0 & 0 & 1 & 0 \end{pmatrix}$. This leads to $M \cdot \vec{\mathbf{S}} = \begin{pmatrix} 1 \\ 1 \\ 0 \\ 0 \end{pmatrix} = \vec{\mathbf{S}}$.

3.2 Experiment

The question now is: “Does the polarization change with every photon BEC and does the duty cycle and power of the pulse influence it and what is it?”. The duty cycle is defined as the product of the repetition rate and the pulse width. To answer this question four different duty cycles are chosen: 2.5×10^{-6} , 2.5×10^{-5} , 6.25×10^{-5} and 1×10^{-4} . For higher duty cycles triplet quenching has been observed. These duty cycles increase the lifetime of the BEC. With each duty cycle the pump power is varied from 0.40 W to 0.80 W in steps of 0.01 W. For each step 100 frames are recorded. This range of pump powers is chosen because it shows a clear transition from thermalization to BEC.

3.2.1 Sequence

To make images of single photon BEC everything has to be carefully timed. A photon BEC is created with a pump laser whose light is chopped up into pulses by acoustic optical modulators (AOMs). During the experiment we will vary the duty cycle. During the experiments the duty cycle is varied by changing the pulse width. The repetition rate will be held constant for all measurements.

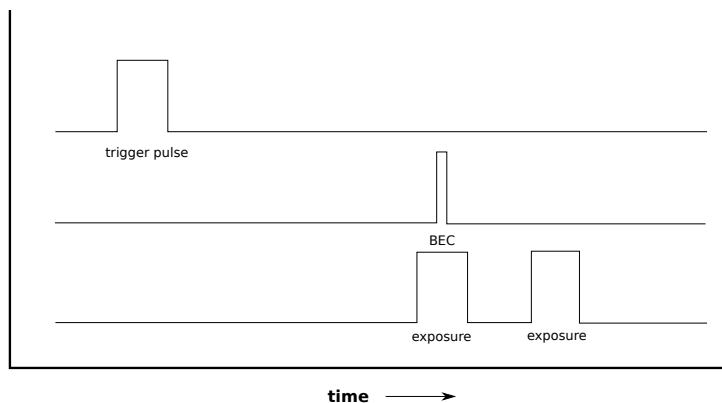


Figure 3.3: The measurement cycle starts with a trigger pulse. This trigger initialises the making of a BEC and the picture thereof. Shortly after the picture of the BEC there is another picture of the background signal.

A measurement cycle starts with a trigger pulse as can be seen in Fig.3.3. This pulse is sent to the camera and to the AOMs. The camera has a response time of 10 ms and a minimum exposure time of 50 μ s. The pulse sent to the AOMs is delayed so that a BEC is created within the time interval that the chip is exposed. A second image is made 30 ms later to record the background signal. The results of such a measurement can be seen in Fig.3.4. Here we see the condensate split into four where each of the signals account for one of the Stokes parameters.

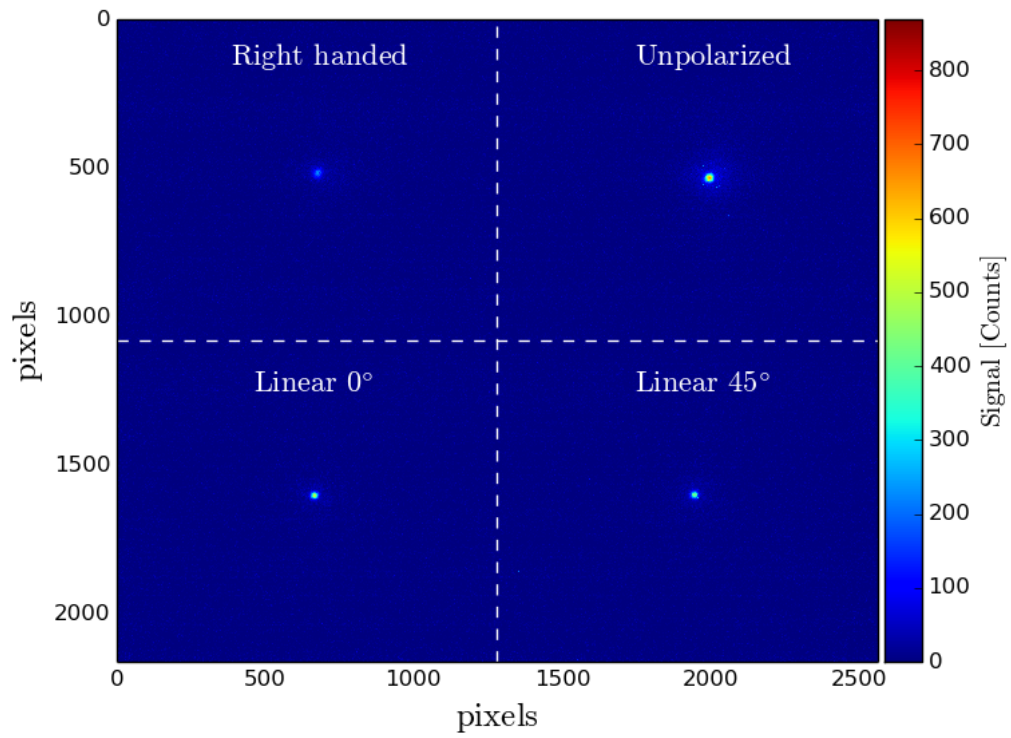


Figure 3.4: An image of a photon BEC. Note that the y -axis is inverted. Each of the four quadrants image one of the Stokes parameters.

4. Results

4.1 Analysis

The data files that we work with are Portable Network Graphics. These are 16-bit deep and uncompressed. These two-dimensional arrays are split into four areas that are depicted in Fig.3.4. The first step is to determine the coordinates of the centres of each of the four signals. This is necessary to relate the signals to one another. This is done separately for each of the four signals. To determine the centre coordinates we start out with an estimate of these coordinates and from that point take a square area that is large enough to encapsulate the signal from the BEC and part of the thermal cloud. With this new array a radial average is made for each pixel and for each a Gaussian function is fitted to that data. From this fit the variance parameter that is found is stored in another array of the same size at its respective location. With this array the mean value is calculated for each column and a parabola is fitted to those results. The minimum value of this fit is the x -coordinate of the centre. To find the y -coordinate the above process is repeated but for rows instead of columns. We treat these coordinates as a better estimate as the previous one. and repeat the entire process forty times for randomly chosen frames The average of those values are used as the centre coordinates for further analysis.

With these coordinates the four signals can be related to one another and the normalized Stokes parameters can be obtained for every pixel using a rewritten form of Eq.2.9

$$S_0 = \frac{I_{\text{tot}}}{I_{\text{tot}}}, \quad S_1 = \frac{2 \times I_{0^\circ}}{I_{\text{tot}}} - 1, \quad S_2 = \frac{2 \times I_{45^\circ}}{I_{\text{tot}}} - 1, \quad S_3 = 1 - \frac{2 \times I_{\text{R}}}{I_{\text{tot}}}.$$

The above equations are used on every pixel separately. These results are then radially averaged and can be represented as in Fig.4.1. In the first three graphs the last three Stokes parameters are plotted. They can vary between plus one and minus one. In the last graph the total polarization is plotted, this is the quadratic sum of the last three Stokes parameters and can only vary between zero and one.

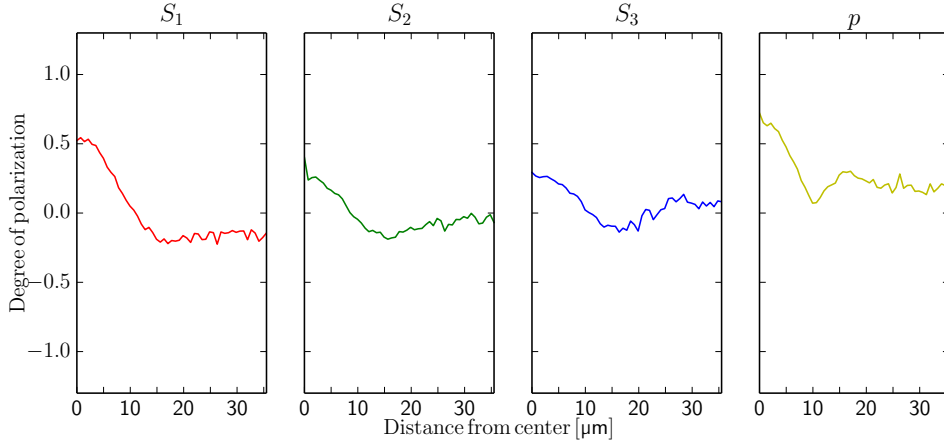


Figure 4.1: Stokes parameters of a single BEC. S_1 has a higher value than S_2 and S_3 indicating that this BEC is mostly LHP. All Stokes parameters decrease to roughly zero. This indicates that the thermal cloud is mostly unpolarized.

4.2 Polarization Measurements

4.2.1 First Duty Cycle

To determine when BEC occurs for duty cycle 2.5×10^{-6} we radially average the intensity from the centre of the unpolarized signal. This is done for all powers and its subsequent frames. For every power the mean is taken over its frames and the results are shown in Fig.4.2. In this figure the top graph shows the radial profiles in a linear scale and in the bottom graph in a semi-log scale. The pump powers used range from 0.40 W to 0.80 W in steps of 0.01 W. Every power is given an offset so they can be studied more clearly. The legend skips every other power to prevent clutter. In this figure it can be seen that for increasing power the radial profile changes. For the lowest pump powers the profiles are straight lines. This is because no Bose-Einstein condensation has occurred. For higher powers it gets a Gaussian bell shape, this is where Bose-Einstein condensation sets in, these are the thicker, dotted lines. After increasing the power beyond this point higher order modes are occupied, this can be seen by the increasing intensity further away from the centre. Or in other words the bell shape gets a hump. This hump can be seen more clearly on the semi-log scale.

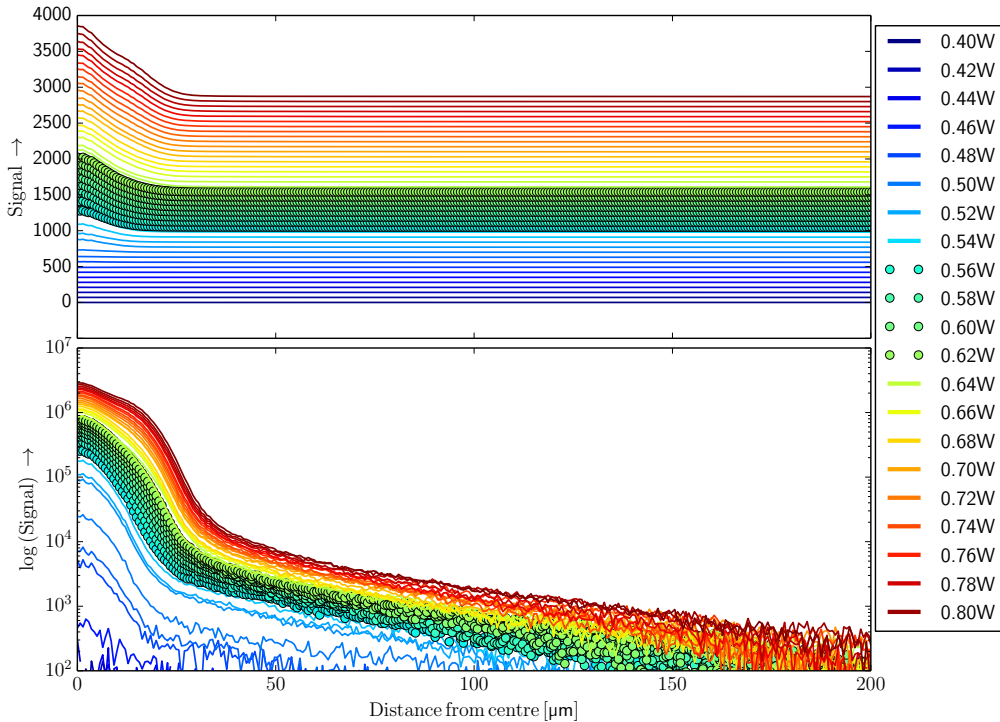


Figure 4.2: Radially averaged intensity profiles for duty cycle 2.5×10^{-6} , with a linear scale on the top graph and on a semi-log scale on the bottom graph. Every subsequent power is given an offset so it can be observed more clearly. The pump powers used range from 0.40 W to 0.80 W in steps of 0.01 W. The legend skips every other power to prevent clutter. The thicker, dotted lines are powers where we reach BECs. For this duty cycle there are eight.

To see if the polarization changes for every BEC and if the power influences it, the Stokes parameters are determined for the centre pixel of all measurements of this duty cycle. The Stokes parameters of this pixel are shown in Fig.4.3. The axis labelled: “Run number” shows increasing powers. The axis labelled: “Frame number” shows the hundred frames taken for each power. For low powers the Stokes parameters seem to be fairly random. For higher powers the Stokes parameters converge to a constant value and does not change for different frames.

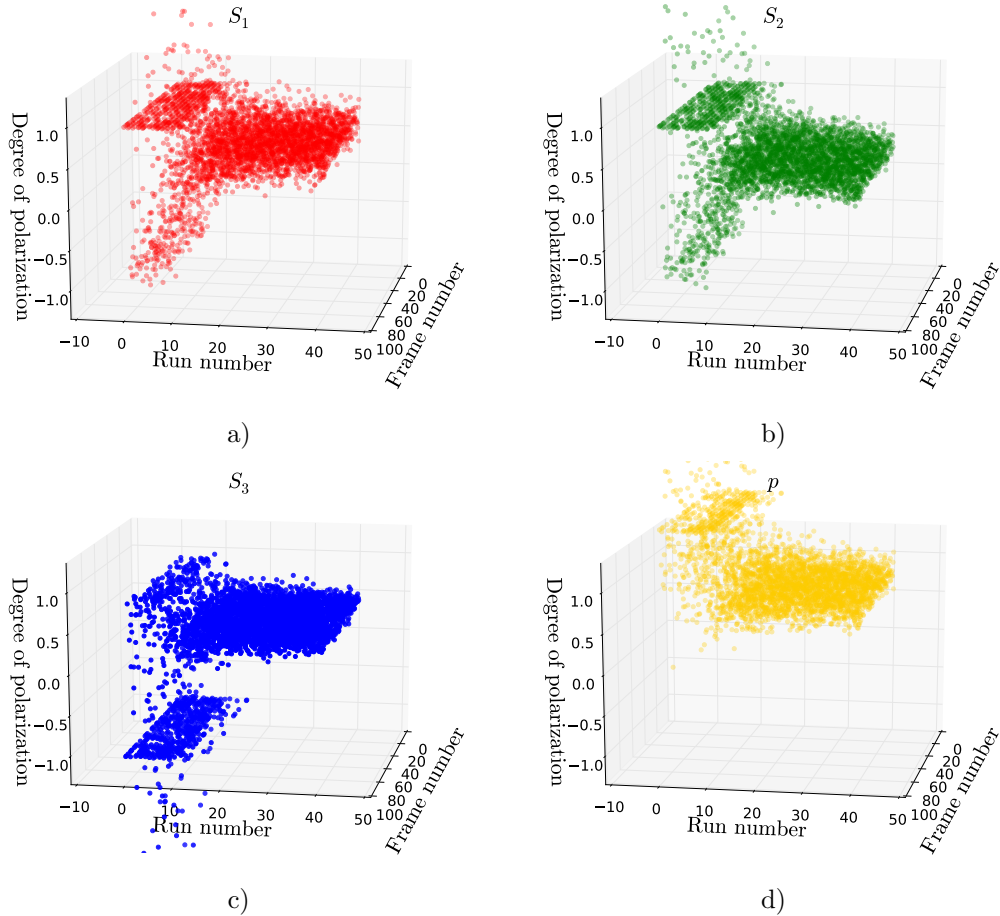


Figure 4.3: The Stokes parameters of the centre coordinate of duty cycle 2.5×10^{-6} for all pump powers and frame numbers. Each run number corresponds to a different pump power in ascending order i.e. in run 0, 0.40 W was used and in run 40, 0.80 W. For low powers the values are quite random. For higher powers the values converge and are very constant for subsequent frames.

The polarization of the centre of a BEC is roughly constant for every BEC that is measured. To check how the rest of the BEC behaves we have determined the radially averaged Stokes parameters of every BEC and taken its average. The results are plotted in Fig.4.4c). The Stokes parameters are very constant over multiple BEC, as can be observed in the figure. S_1 starts at around 0.6, this means that it is mostly LHP. S_2 starts at 0.5 thus the BEC contains more L+45P than L-45P. The BEC is also slightly LCP because S_3 starts at around 0.4. The total polarization p starts

at 0.9 thus the BEC starts out almost completely polarized. From the initial values the Stokes parameters and the total polarization slowly decrease towards zero. Thus the thermal cloud seems to be unpolarized. At around $13\ \mu\text{m}$ the Stokes parameters diverge. This is at the edge of the thermal cloud. The reason it diverges at this location is that the normalization process does not work properly anymore. This is because we only measure background radiation from that point forward thus we are dividing random numbers by random numbers.

In Fig.4.4a) there is an image of the unpolarized signal of a BEC. In b) the averaged radial profile is plotted of the respective BEC. The circle in a) and the dotted line in b) and c) indicate the size of the BEC. This size was determined by using a fit procedure especially designed for the radial intensity profiles of BECs. One of the fit parameters is the size of the BEC.

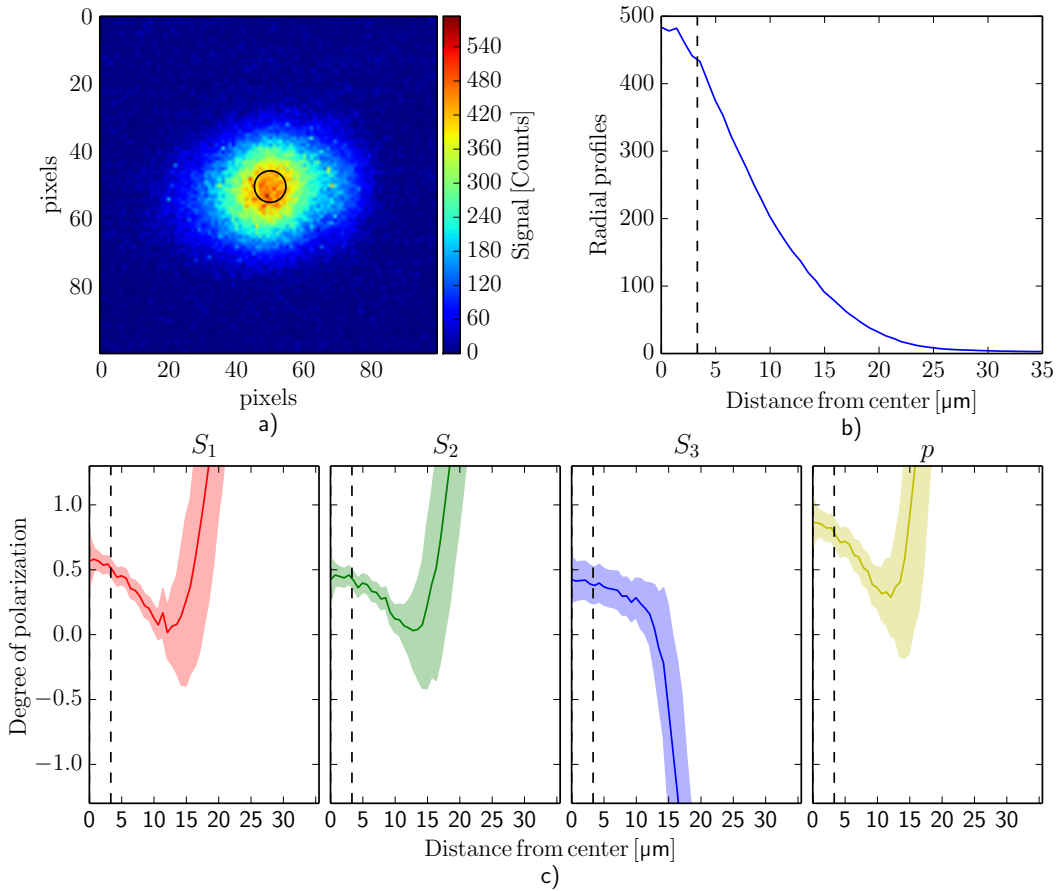


Figure 4.4: a) Image of the unpolarized signal of a single BEC, the ring indicates the size of the BEC. b) Radially averaged intensity distribution taken over a hundred frames of the same BEC in a). The dotted line indicates the radius of the BEC. c) The mean value of the Stokes parameters of duty cycle 2.5×10^{-6} taken over eight different powers. The dotted line again indicates the radius of the BEC. The thermal cloud ends at around $13\ \mu\text{m}$, this is the reason the Stokes parameters diverge because the normalization does not work properly anymore.

4.2.2 Second Duty Cycle

The data for duty cycle 2.5×10^{-5} are analysed in the same way as in Section 4.2.1. Fig.4.5 shows that for the lowest eight pump powers Bose-Einstein condensation occurs. These are again indicated by the thicker, dotted lines. For pump powers higher than 0.47 W we observe higher order modes.

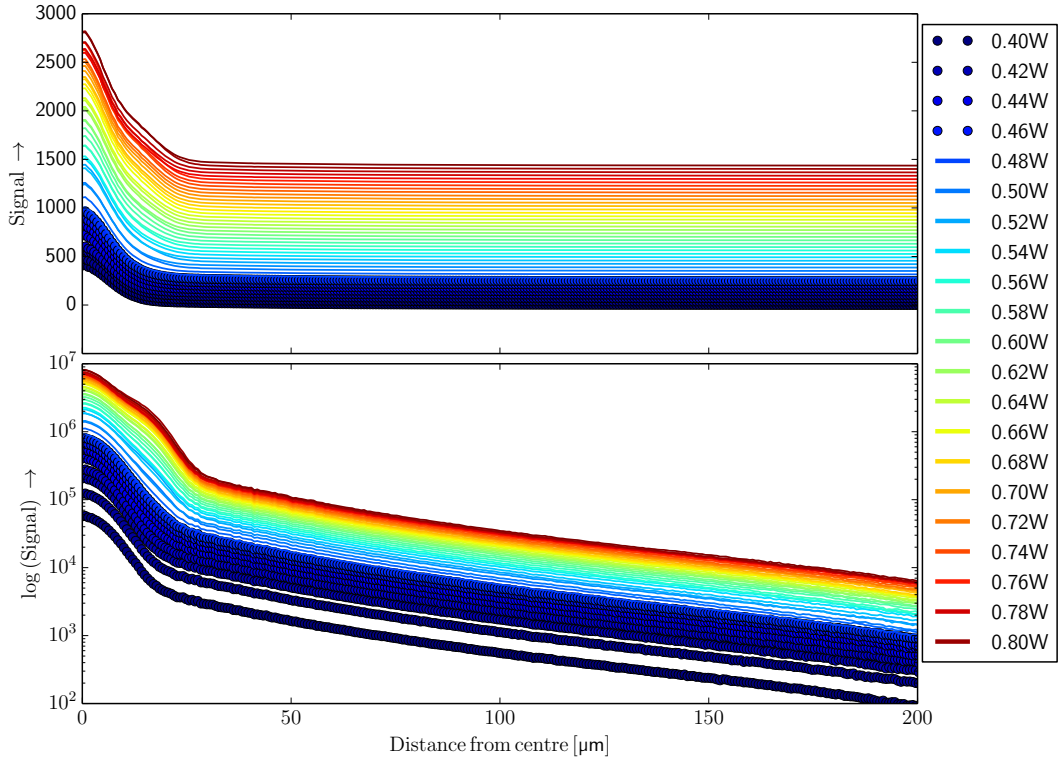


Figure 4.5: Radially averaged intensity profiles for duty cycle 2.5×10^{-5} , with a linear scale on the top graph and on a semi-log scale on the bottom graph. Every subsequent power is given an offset so it can be observed more clearly. The pump powers used range from 0.40 W to 0.80 W in steps of 0.01 W. The legend skips every other power to prevent clutter. The thicker, dotted lines are powers where we reach BECs. For this duty cycle there are eight.

Fig.4.6 shows four fairly stable plateaus. There are no measurements of the Stokes parameters without BEC or higher order modes. This is due to achieving condensation for the lowest pump power that was used. This figure clearly shows that the polarization in the centre of the trap is very constant for every newly created BEC and even higher order modes.

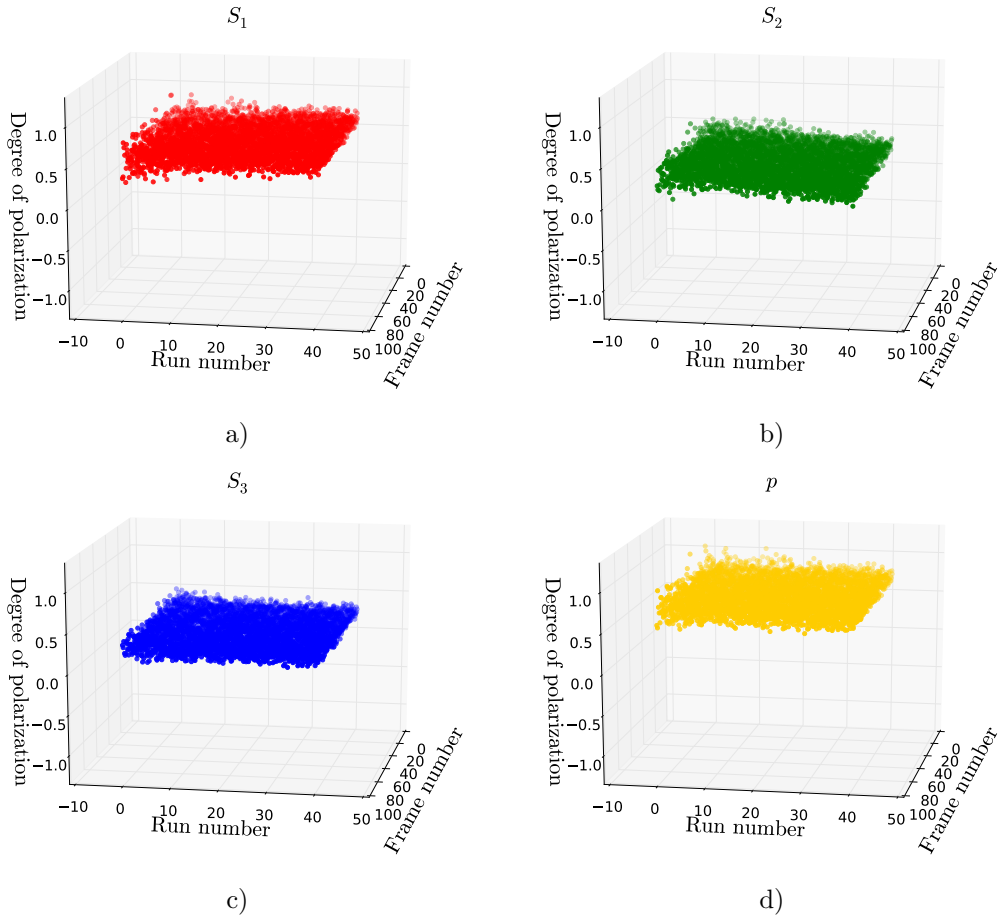


Figure 4.6: The Stokes parameters of the centre coordinate of duty cycle 2.5×10^{-5} for all powers and frame numbers. Each run number corresponds to a different pump power in ascending order i.e. run 0 is 0.40 W and run 40 is 0.80 W. There are no measurements of the Stokes parameters where there is no BEC because condensation was achieved for the lowest pump power used.

We again determine the radially averaged Stokes parameters of every BEC and take the average over all eight-hundred of them. The results are shown in Fig.4.7c). The results are similar to Fig.4.4, they are again very constant. S_1 has the highest value of all three Stokes parameters indicating that the BEC is primarily LHP. There is again more L+45P light than L-45P light and the BECs are slightly LCP. The Stokes parameters decreasing to roughly zero indicate that the thermal cloud is unpolarized. The thermal cloud is slightly bigger for this duty cycle ending at roughly $20\ \mu\text{m}$ than the previous duty cycle. This edge is indicated by the divergence of the Stokes parameters.

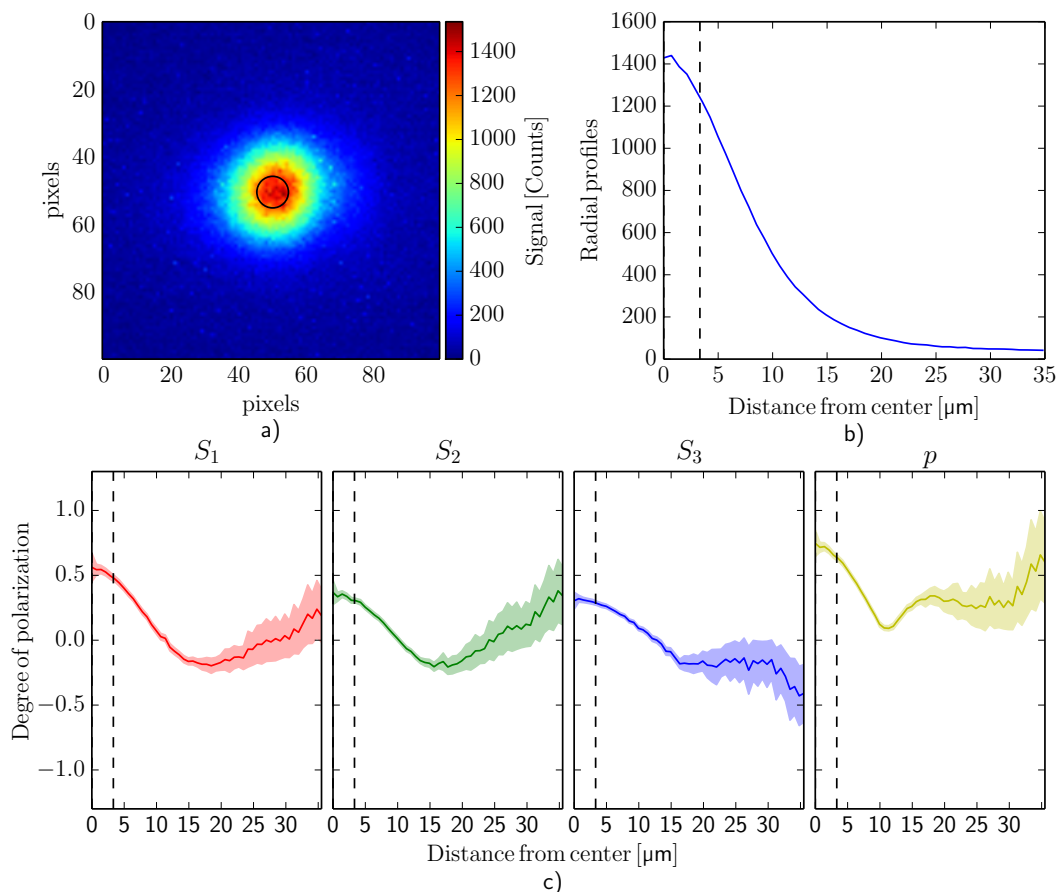


Figure 4.7: a) Image of the unpolarized signal of a single BEC, the ring indicates the size of the BEC. b) Radially averaged intensity distribution taken over a hundred frames of the same BEC in a). The dotted line indicates the radius of the BEC. c) The mean value of the Stokes parameters of duty cycle 2.5×10^{-5} taken over eight different powers. The dotted line again indicates the radius of the BEC. The thermal cloud ends around $20\ \mu\text{m}$, this is the reason the Stokes parameters diverge because the normalization does not work properly any more.

4.2.3 Third Duty Cycle

The data for duty cycle 6.25×10^{-5} are analysed in the same way as in Section 4.2.1 & 4.2.2. In Fig. 4.8 it can be seen that condensation sets in for the highest five pump powers. These pump powers are indicated by the thicker, dotted red lines. For these measurements higher order modes are not observed.

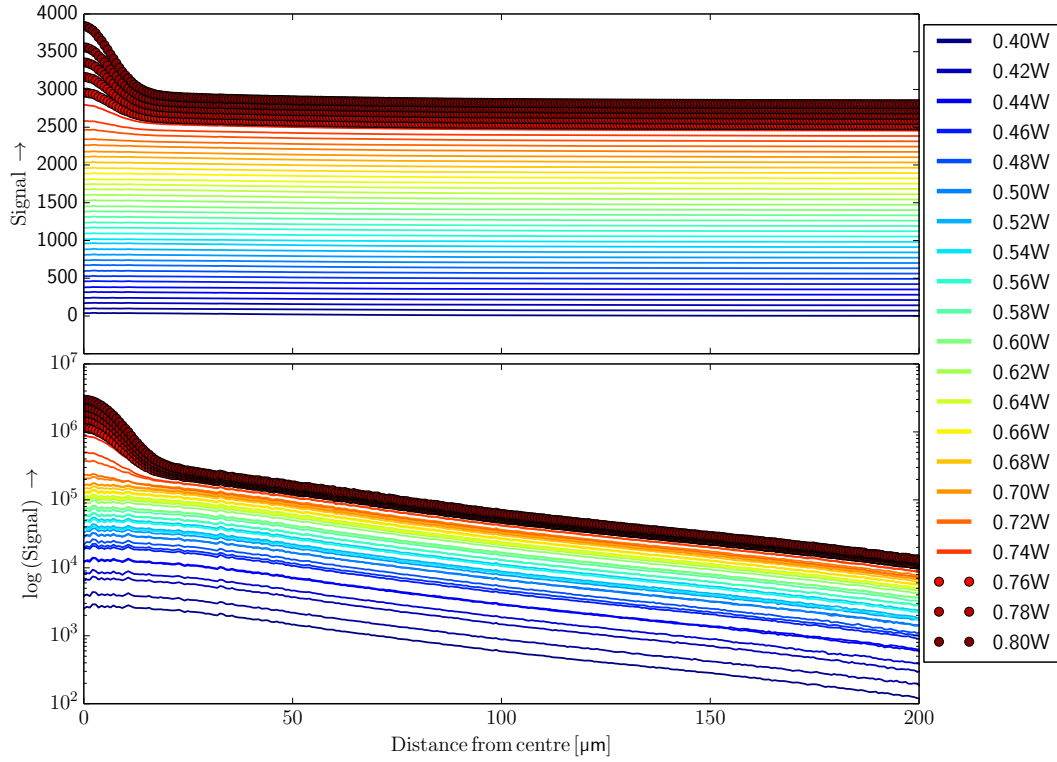


Figure 4.8: Radially averaged intensity profiles for duty cycle 6.25×10^{-5} , with a linear scale on the top graph and on a semi-log scale on the bottom graph. Every subsequent power is given an offset so it can be observed more clearly. The pump powers used range from 0.40 W to 0.80 W in steps of 0.01 W. The legend skips every other power to prevent clutter. The thicker, dotted lines are powers where we reach BECs. For this duty cycle there are five.

In Fig.4.9 the Stokes parameters of the centre of the trap are plotted. The values for the Stokes parameters are quite random for most measurements, but it shows clear convergence to a constant value for higher pump powers when BEC is achieved.

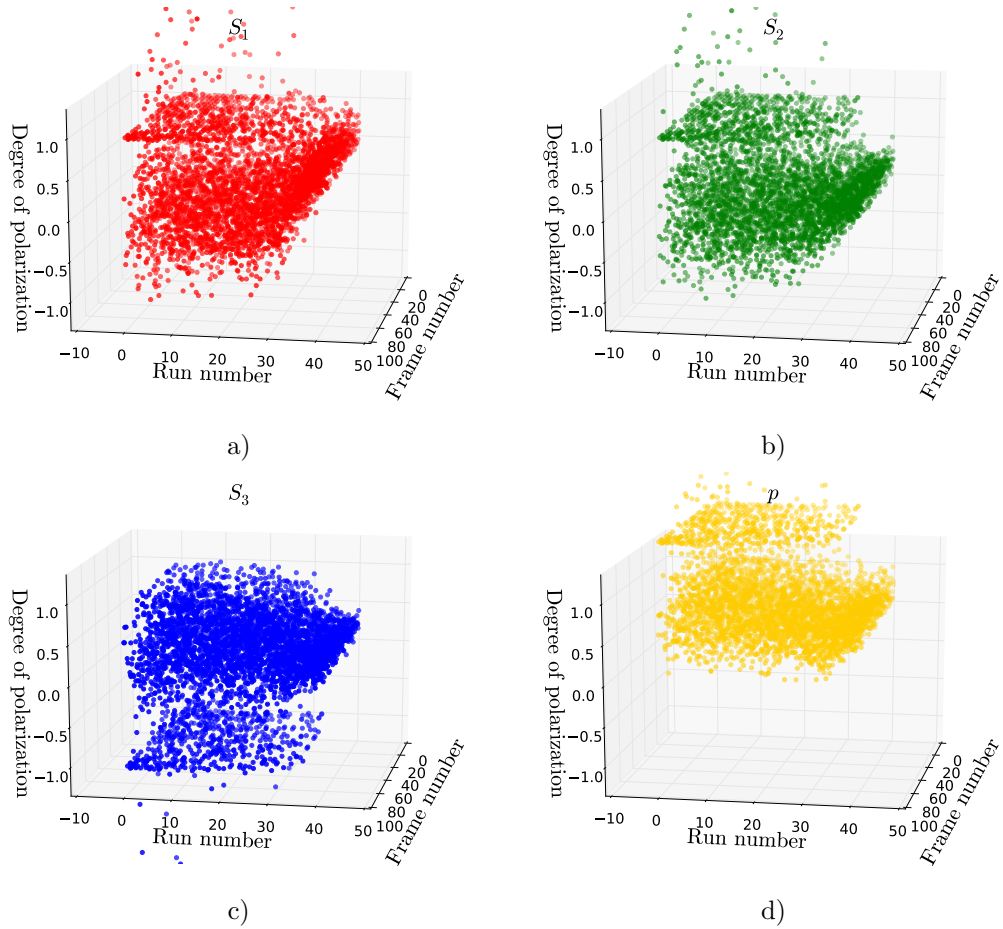


Figure 4.9: The Stokes parameters of the centre coordinate of duty cycle 6.25×10^{-5} for all powers and frame numbers. Each run number corresponds to a different pump power in ascending order i.e. in run 0, 0.40 W was used and in run 40, 0.80 W. The Stokes parameters look quite random for most of the measurement, but it still clearly converges to a constant value for the highest used pump powers.

The mean of the radially averaged Stokes parameters of all five-hundred BECs is determined and the results are presented in Fig.4.10c). The results are again very constant and similar to the previous results. It again shows that the BECs are mostly LHP and the thermal cloud is roughly unpolarized. This is the first measurement where there is no divergence of the Stokes parameters in the region that is plotted. This is because the radius we consider is not larger than the thermal cloud.

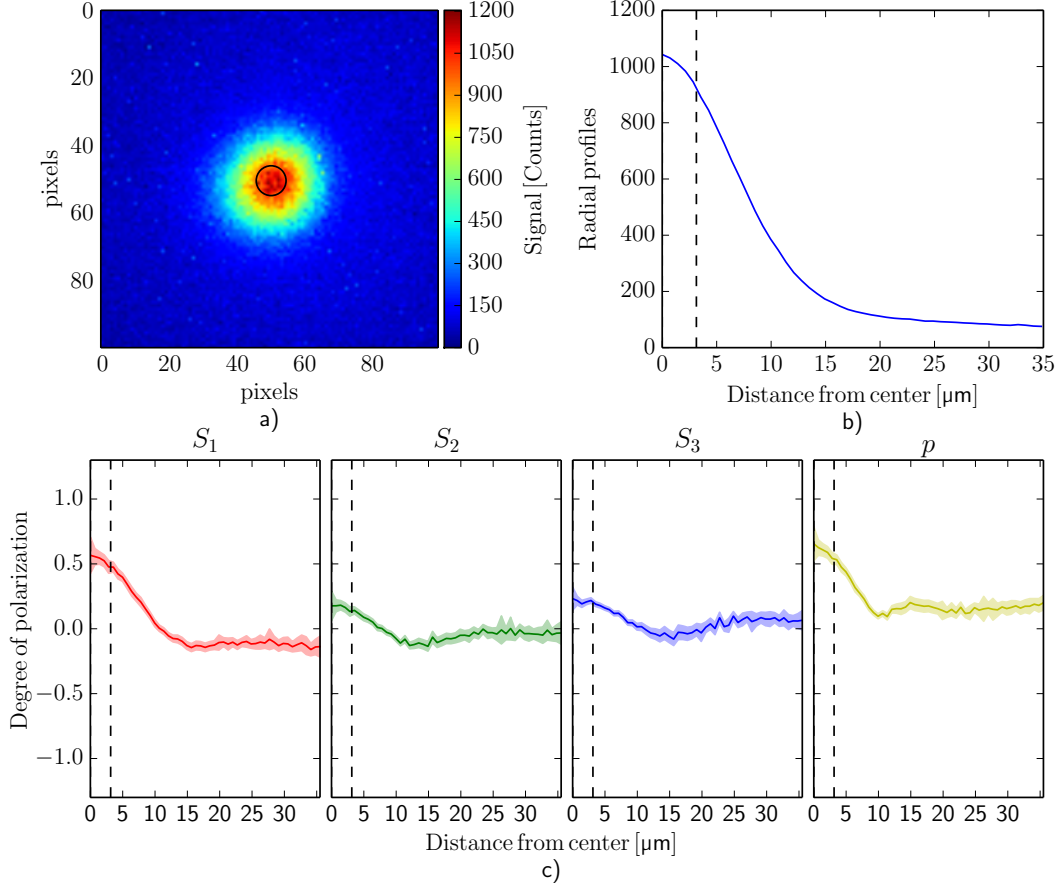


Figure 4.10: a) Image of the unpolarized signal of a single BEC, the ring indicates the size of the BEC. b) Radially averaged intensity distribution taken over a hundred frames of the same BEC in a). The dotted line indicates the radius of the BEC. c) The mean value of the Stokes parameters of duty cycle 6.25×10^{-5} taken over five different powers. The dotted line again indicates the radius of the BEC.

4.2.4 Fourth Duty Cycle

The data collected from duty cycle 1×10^{-4} are analysed in the same way as in Section 4.2.1, 4.2.2 & 4.2.3. Fig.4.11 shows the radial profiles from this duty cycle. Bose-Einstein condensation sets in at a pump power of 0.65 W and the subsequent powers are indicated by the thicker, dotted lines.

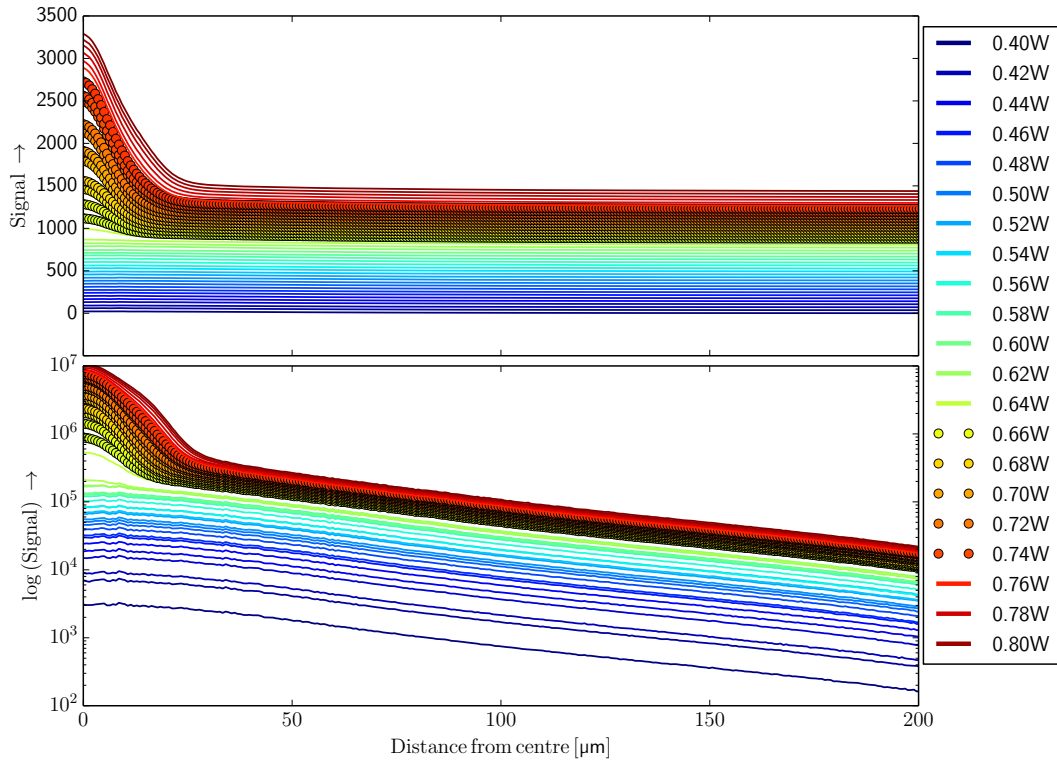


Figure 4.11: Radially averaged intensity profiles for duty cycle 1×10^{-4} , with a linear scale on the top graph and on a semi-log scale on the bottom graph. Every subsequent power is given an offset so it can be observed more clearly. The pump powers used range from 0.40 W to 0.80 W in steps of 0.01 W. The legend skips every other power to prevent clutter. The thicker, dotted lines are powers where we reach BECs. For this duty cycle there are eleven.

The Stokes parameters of the centre of the trap are plotted in Fig.4.12. They are again quite random for pump powers where BEC is not yet achieved and converge nicely for when it is.

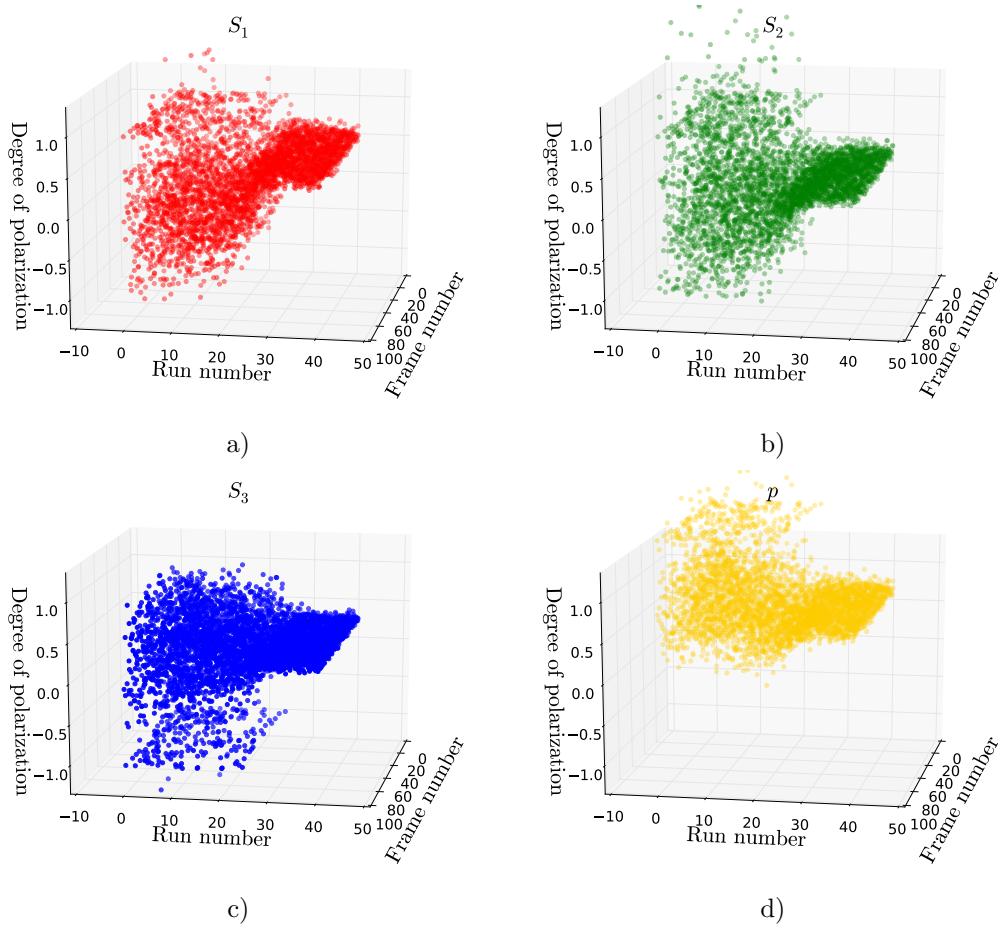


Figure 4.12: The Stokes parameters of the centre coordinate of duty cycle 1×10^{-4} for all powers and frame numbers. For low powers the values are quite random, for higher powers the values converge and are very constant for subsequent frames.

This time the mean of the radially averaged Stokes parameters is taken over eleven-hundred BECs and plotted in Fig.4.13c). The standard deviation of the mean is again very narrow indicating that the polarization of every newly created BEC is roughly the same. The polarization of the BEC is like the other duty cycles again mostly LHP. But also a bit L+45P and LCP. The Stokes parameters also decrease slowly like before and the thermal cloud is roughly unpolarized.

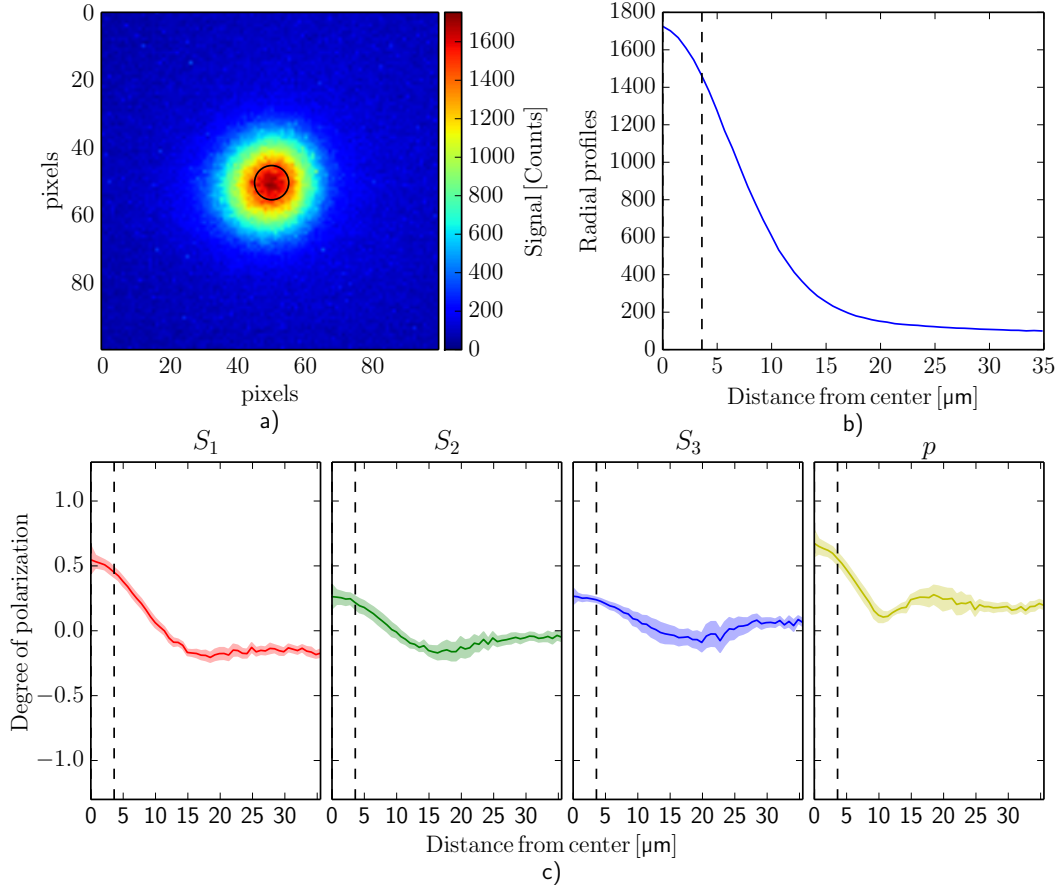


Figure 4.13: a) Image of the unpolarized signal of a single BEC, the ring indicates the size of the BEC. b) Radially averaged intensity distribution taken over a hundred frames of the same BEC in a). The dotted line indicates the radius of the BEC. c) The mean value of the Stokes parameters of duty cycle 1×10^{-4} taken over eight different powers. The dotted line again indicates the radius of the BEC.

Using Eq.2.10 and the values found in Fig.4.13 the polarization ellipse can be constructed. This is done for the BEC and the thermal cloud and is shown in Fig.4.14. The polarization ellipse for the thermal cloud is nearly non existing because the major-axis of this ellipse scales linearly with the total polarization p of the signal. As can be seen in Fig.4.13c) p is nearly zero.

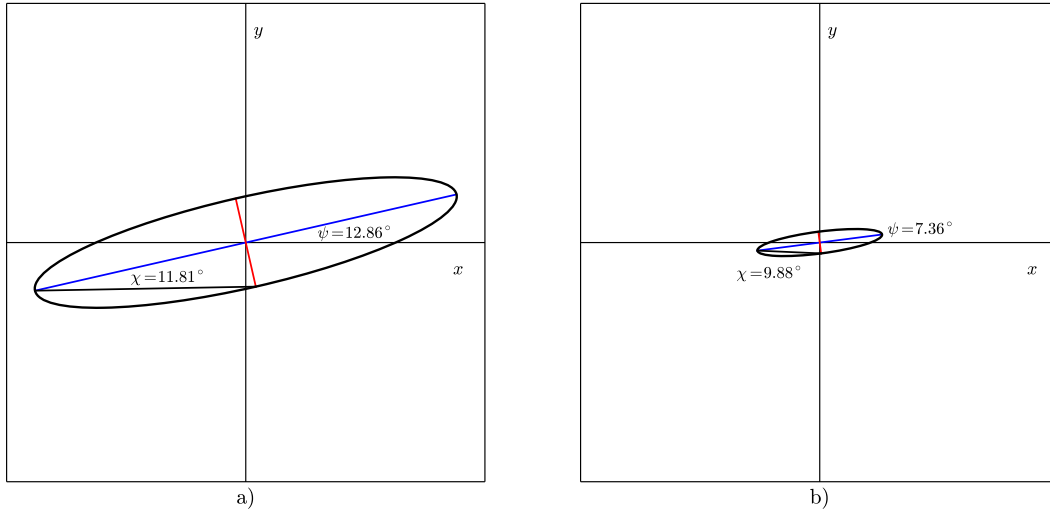


Figure 4.14: a) Polarization ellipse of the Photon BEC. b) Polarization ellipse of the thermal cloud. The major-axis of the ellipse scales linearly with the total polarization of the signal. Because the signal from the thermal cloud is nearly zero, the polarization ellipse in b) is nearly non-existent.

5. Conclusion

We started out by asking if the polarization of every newly created photon BEC was randomly chosen, and whether the power and/or duty cycle influences it. We also asked what the polarization of a photon BEC is. To answer these questions we recorded images of single BECs for different pump powers and duty cycles and determined the Stokes parameters of every BEC. We found that the polarization is fixed. It does not change for BECs made with the same pump power or different pump powers. The duty cycle also does not influence it.

We also found that the photon BEC has a clear polarization compared to the thermal cloud. It shows a superposition of multiple polarization states with a strong contribution of the linearly horizontally polarized state. Although there is some uncertainty in what the polarization is exactly. We did not include the effect of the setup on the polarization of the signal. This is due to difficulties with the calibration measurements that were not resolved at the time of writing this thesis.

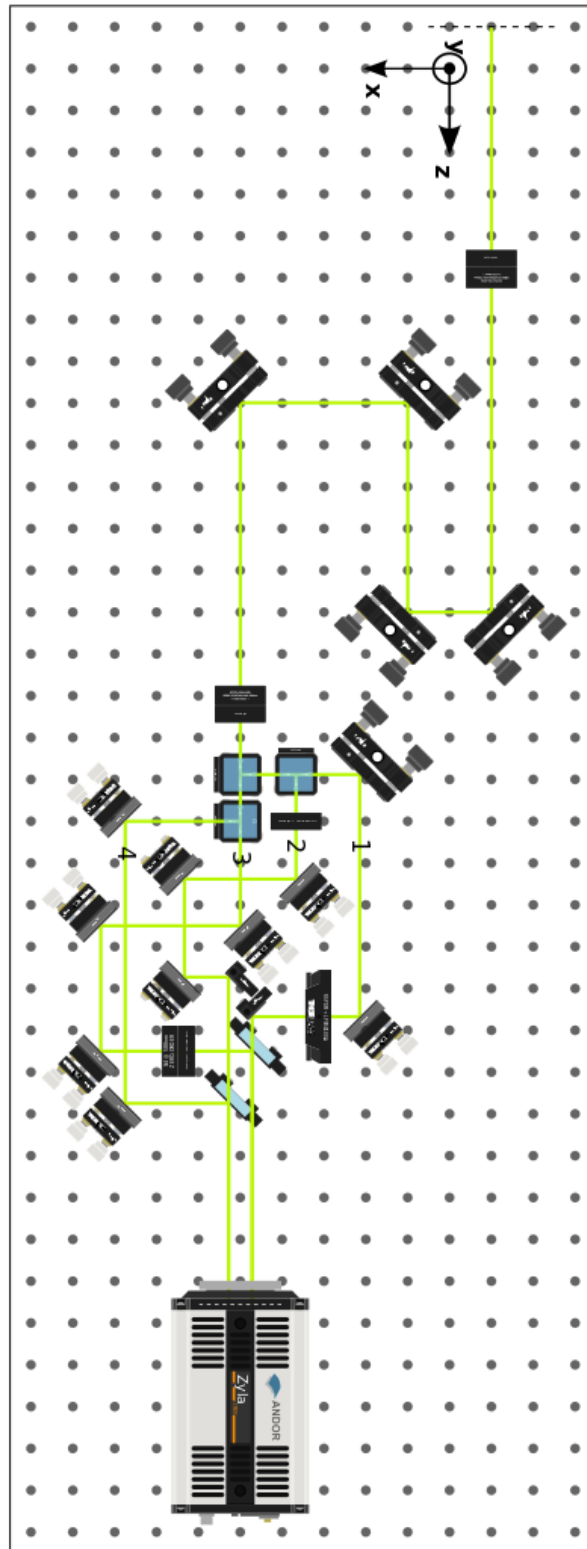
At present there is no clear idea why this polarization is pinned down and what it is pinned down by. A hypothesis is that it is due to the polarization of the pump laser. Another hypothesis is that it is due to an anisotropy of the cavity. These are both good starting points for future research that can be done on this subject.

Another option for the future is using the polarization measurement setup for other experiments. The strength of this setup is that it can measure the polarization of a signal with a lifetime of the order of microseconds, and it can measure this in rapid succession.

Acknowledgement



First of all let me thank Dr. Dries van Oosten to have given me the opportunity to work on such an exciting new subject. Second I would like to thank Sebastiaan Greveling who supervised me on a daily basis. Your work ethic is admiring and your enthusiasm for experimental physics is very contagious. Your door was always open and I think we found a good balance between work and just messing around. I would also like to thank Marcel Scholten who was always willing to answer my questions and on occasion point out faults in my code. I also enjoyed our discussions about life, the universe and everything. Lastly I would like to thank everyone of the Nanophotonics group for making me feel welcome and part of the group immediately. I enjoyed all your company immensely and I like to think that I made some new friends in the short time I was there.

Appendix A. Schematic



Appendix B. Part List

image	description	name
	<ul style="list-style-type: none"> • camera 	<ul style="list-style-type: none"> • Andor Zyla 5.5 sCMOS
	<ul style="list-style-type: none"> • compact kinematic mount • non-polarizing beamsplitter cube 	<ul style="list-style-type: none"> • KMS/M • BS010
	<ul style="list-style-type: none"> • compact kinematic mount • mirror holder • mirror 	<ul style="list-style-type: none"> • KMS/M • KMSS/M • MH25 • BB1-E02
	<ul style="list-style-type: none"> • D-mirror holder • D-mirror 	<ul style="list-style-type: none"> • DMM1/M • BBD1-E02
	<ul style="list-style-type: none"> • lens holder • lens $f = 150\text{mm}$ • lens $f = 500\text{mm}$ 	<ul style="list-style-type: none"> • LMR1/M • AC254-150-A-ML • AC254-500-A-ML

image	description	name
	<ul style="list-style-type: none"> • rotation mount • linear polarizer 	<ul style="list-style-type: none"> • RSP1/M • LPVISE100-A
	<ul style="list-style-type: none"> • lens holder • linear polarizer • quarter waveplate 	<ul style="list-style-type: none"> • LMR1/M • LPVISE100-A • $\frac{\lambda}{4}$ @ 588 nm ZERO-ORDER

References

- ¹A. Zannoni, “On the Quantization of the Monoatomic Ideal Gas”, ArXiv eprint (1999).
- ²S. J. Blundell and K. M. Blundell, *Concepts in thermal physics* (Oxford University Press, 2010) Chap. 29, pp. 355–357.
- ³S. Bose, “Plancks gesetz und lichtquantenhypothese”, *Zeitschrift für Physik* **26**, 178–181 (1924).
- ⁴M. H. Anderson, J. R. Ensher, M. R. Matthews, C. E. Wieman, and E. A. Cornell, “Observation of bose-einstein condensation in a dilute atomic vapor”, *Science* **269**, 198–201 (1995).
- ⁵S. J. Blundell and K. M. Blundell, *Concepts in thermal physics* (Oxford University Press, 2010) Chap. 23, pp. 270–273.
- ⁶Y. Zel’dovich and E. Levich, “Bose condensation and shock waves in photon spectra”, *Journal of Experimental and Theoretical Physics* **82** (1969).
- ⁷R. Y. Chiao and J. Boyce, “Bogoliubov dispersion relation and the possibility of superfluidity for weakly interacting photons in a two-dimensional photon fluid”, *Phys. Rev. A* **60**, 4114–4121 (1999).
- ⁸C. R.Y., “Bogoliubov dispersion relation for a ‘photon fluid’: is this a superfluid?”, *Optics Communications* **179**, 157–166 (2000).
- ⁹M. W. Mitchell, C. I. Hancox, and R. Y. Chiao, “Dynamics of atom-mediated photon-photon scattering”, *Phys. Rev. A* **62**, 043819 (2000).
- ¹⁰E. L. Bolda, R. Y. Chiao, and W. H. Zurek, “Dissipative optical flow in a nonlinear fabry-pérot cavity”, *Phys. Rev. Lett.* **86**, 416–419 (2001).
- ¹¹C. F. McCormick, R. Y. Chiao, and J. M. Hickmann, “Weak-wave advancement in nearly collinear four-wave mixing”, *Opt. Express* **10**, 581–585 (2002).
- ¹²J. P. Torres, A. Alexandrescu, and L. Torner, “Quantum spiral bandwidth of entangled two-photon states”, *Phys. Rev. A* **68**, 050301 (2003).
- ¹³R. Y. Chiao, T. H. Hansson, J. M. Leinaas, and S. Viefers, “Effective photon-photon interaction in a two-dimensional “photon fluid””, *Phys. Rev. A* **69**, 063816 (2004).
- ¹⁴J. C. Martinez and Anton, “Semiclassical quantization of the electromagnetic field confined in a kerr-effect nonlinear cavity”, *J. Opt. Soc. Am. B* **23**, 1644–1649 (2006).
- ¹⁵B. T. Seaman and M. J. Holland, “Evaporative Cooling of a Photon Fluid to Quantum Degeneracy”, ArXiv e-prints (2008).
- ¹⁶C. Connaughton, C. Josserand, A. Picozzi, Y. Pomeau, and S. Rica, “Condensation of classical nonlinear waves”, *Phys. Rev. Lett.* **95**, 263901 (2005).
- ¹⁷J. Kasprzak, M. Richard, S. Kundermann, A. Baas, P. Jeambrun, J. M. J. Keeling, F. M. Marchetti, M. H. Szymanska, R. Andre, J. L. Staehli, V. Savona, P. B. Littlewood, B. Deveaud, and L. S. Dang, “Bose-einstein condensation of exciton polaritons”, *Nature* **443**, 409–414 (2006).

- ¹⁸R. Balili, V. Hartwell, D. Snoke, L. Pfeiffer, and K. West, “Bose-einstein condensation of microcavity polaritons in a trap”, *Science* **316**, 1007–1010 (2007).
- ¹⁹J. Kasprzak, M. Richard, A. Baas, B. Deveaud, R. André, J.-P. Poizat, and L. S. Dang, “Second-order time correlations within a polariton bose-einstein condensate in a cdte microcavity”, *Phys. Rev. Lett.* **100**, 067402 (2008).
- ²⁰J. Kasprzak, D. D. Solnyshkov, R. André, L. S. Dang, and G. Malpuech, “Formation of an exciton polariton condensate: thermodynamic versus kinetic regimes”, *Phys. Rev. Lett.* **101**, 146404 (2008).
- ²¹K. G. Lagoudakis, M. Wouters, M. Richard, A. Baas, I. Carusotto, R. Andre, L. S. Dang, and B. Deveaud-Pledran, “Quantized vortices in an exciton-polariton condensate”, *Nature Physics* **4**, 706–710 (2008).
- ²²A. Amp, J. Lefrere, S. Pigeon, C. Adrados, C. Ciuti, I. Carusotto, R. Houdre, E. Giacobino, and A. Bramati, “Superfluidity of polaritons in semiconductor microcavities”, *Nature Physics* **5**, 805–810 (2009).
- ²³T. Byrnes, K. N. Y., and Y. Yamamoto, “Exciton-polariton condensates”, *Nature Physics* **10**, 803–813 (2014).
- ²⁴J. Klaers, F. Vewinger, and M. Weitz, “Thermalization of a two-dimensional photonic gas in a ‘white wall’ photon box”, *Nature Physics* **6**, 512–515 (2010).
- ²⁵J. Klaers, J. Schmitt, F. Vewinger, and M. Weitz, “Bose-einstein condensation of photons in an optical microcavity”, *Nature* **468**, 545–5548 (2010).
- ²⁶J. Klaers, J. Schmitt, T. Damm, F. Vewinger, and M. Weitz, “Bose-Einstein condensation of paraxial light”, *Applied Physics B: Lasers and Optics* **105**, 17–33 (2011).
- ²⁷D. Griffiths, *Introduction to electrodynamics* (Pearson, 2010) Chap. 9, pp. 387–403.
- ²⁸S. Joardar, *Polarimetry*, <http://www.gmrt.ncra.tifr.res.in/~joardar/lecHtmlPages/lectures/03-Polarimetry.pdf>.
- ²⁹L. Nahon and C. Alcaraz, *Introduction to polarization and stokes parameters determination : case of the vuv*, <http://www.synchrotron-soleil.fr/images/File/soleil/ToutesActualites/Archives-Workshops/2001/circpol-2001/pdf/Laurent-Nahon.pdf>.
- ³⁰*Optical calculus an mueller matrix polarimetry*, <http://prrr.hec.gov.pk/chapters/2067-2.pdf>.
- ³¹*The poincaré sphere*, <http://www.hp1.hp.com/hpjournal/95feb/feb95a4b.pdf>.
- ³²H. Berry, G. Gabrielse, and A. Livingston, “Measurement of the stokes parameters of light”, *Applied Optics* **16**, 3200–3205 (1977).